Influence of the Convergence Angle on the Morphodynamics of Discordant Bed Confluences

Sebastián Guillén Ludeña
PhD Student, Instituto Superior Técnico, TULisbon, Portugal & Laboratory of Hydraulic Constructions, EPFLausanne, Switzerland. Email: sebastian.ludena@epfl.ch

Mário J. Franca
Research and Teaching Associate, *Laboratory of Hydraulic Construction, ÉcolePolytechniqueFédérale de Lausanne EPFL, Switzerland.Email: mario.franca@epfl.ch*

Anton J. Schleiss
Full Professor, *Laboratory of Hydraulic Construction, École Polytechnique Fédérale de Lausanne EPFL, Switzerland. Email: anton.schleiss@epfl.ch*

António H. Cardoso
Full Professor, *Instituto Superior Técnico de Lisboa, Portugal. Email: antonio.cardoso@ist.utl.pt*

ABSTRACT: Within the fluvial network, confluences are particular areas characterized by great ecological value where flow dynamics and bed morphology are much influenced by local patterns. The aim of this article is to describe the influence of the convergence angle on the morphology and hydrodynamics at river channel confluences, where the tributary bed level is higher than the main channel bed (discordant bed). For that purpose, experiments were carried out in a laboratory flume running three discharge ratio scenarios for two different convergence angles (70 and 90 degrees). The tests were run until equilibrium was reached, i.e. when the outgoing solid discharge was equal or larger than 90% of the incoming. Once the bed topography remained stable, bed and water level surfaces were measured. As a result of these tests, and based on the performed measurements, the convergence angle is identified as an important parameter that influences the main-channel bed morphology features and the water level by modifying the shape and position of the main morphological and flow features. Also, the influence of the discharge ratio ($Q_r = Q_t / Q_m$) on these modifications is observed and evaluated.

KEY WORDS: Discordant bed, River confluences, Sediment transport, Morphodynamic, Convergence angle.

1 INTRODUCTION

During the last century, many river training works were carried out with the aim of satisfying societal needs, i.e. aiming at flood protection, human and industrial water supply or irrigation. Along this process, many environmental aspects were neglected causing several and important impacts on the fluvial ecosystems,mostly throughimportant morphological changes.Nowadays, many tributaries are environmentally disconnected from the main river due to channelization works.To rehabilitate the original environment at river confluences, it is essential thus to deepen the knowledge of the hydro-mophodynamic processes at these key areas.

The hydrodynamics of river confluences isreasonably well known. Previous authors performed physical and numerical experiments which allowedthe development of conceptual models to describe the different flow features observed at confluences. Best (1987)described the flow in river confluences by a scheme in which there are six main zones, corresponding to: flow deflection, flow stagnation, flow separation or recirculation zone, maximum velocity, shear layer and flow recovery zone (see Figure 1).

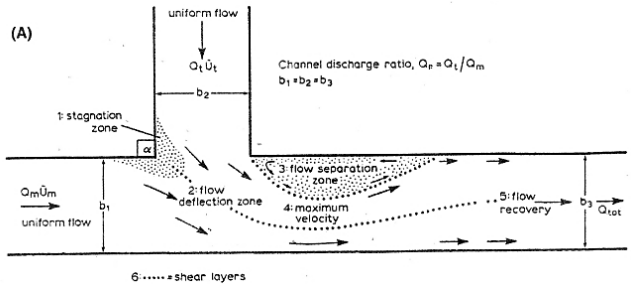

Figure 1 Best's (1987) model of flow dynamics at river channel confluences.

Weber et al. (2001)characterized the 3D flow dynamic patterns based on experiments in a 90º confluence channel with fixed and concordant bed. A three-dimensional shape of the flow separation zone (smaller at the bottom) and a warped shear surface were identified for equally wide tributary and main channel.

Others authors analyzed the existence of a secondary flow consisting in two helical cells (Mosley, 1976). This secondary circulation was confirmed by means of experimental work(Fujita & Komura, 1989), field data (Rhoads & Kenworthy, 1997) and numerical results(Bradbrook, Biron, Lane, Richards, & Roy, 1998). However, the secondary flow depend on the bed concordance and the plane form curvature(Bradbrook et al., 2001; Biron et al., 2002) and, in riverswith large width/depth ratios, no secondary circulation exists given the weaker increase of the water level due to the junction (Parsons et al., 2007).

Biron et al. (1996)analyzed the effects of discordant bed onthe flow dynamicsat open channel confluences (Figure 2). Their facility consisted of a confluence model with a 30º confluence angle in which the main and tributary channels were 0.12 m and 0.08 m wide respectively. The post-confluence channel was 0.15 m wide to avoid a significant increase in Froude number.

As results of these tests, Biron et al. (1996) concluded by the absence of flow deflection near the bed. Moreover, the discordant bed morphology caused the absence of a flow separation zone at the downstream corner of the confluence and the reduction of the flow acceleration zone in the post-confluence. These last effects created an upwelling flow at the downstream junction corner (see Figure2b above).

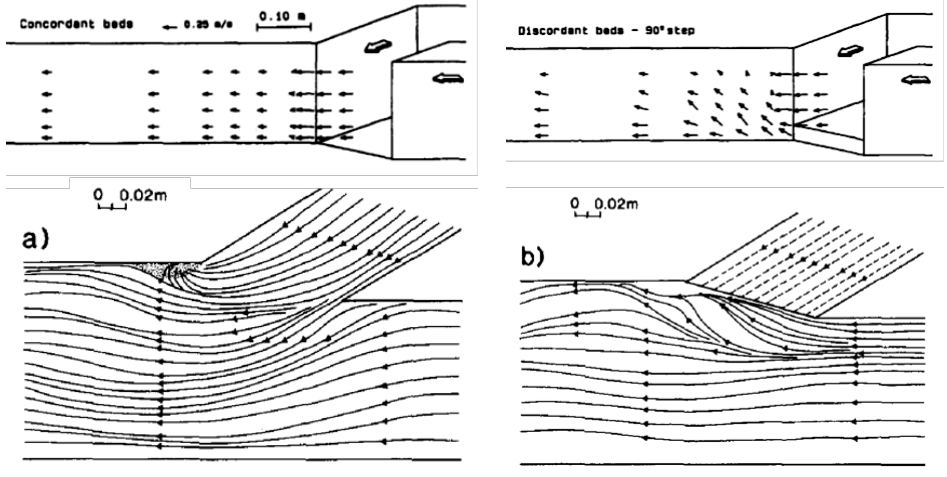

Figure 2 Effects of discordant bed on flow dynamic of channel confluences (P. Biron et al., 1996).(a) Concordant bed horizontal velocity vectors along longitudinal section (above) and bed streamlines (below). (b) Discordant bed horizontal velocity vectors along longitudinal section (above) and bed streamlines (below). Notice the absence of flow defection zone in the streamlines and the signature of upwelling flow in the longitudinal section for discordant bed.

However, few laboratory experiments were carried out under mobile bed conditions.These include the studies ofMosley(1976), Best (1988),Best and Rhoads (2008),Leite Ribeiro, (2011) and Leite Ribeiro et al., (2012a; b). Most of the developed morphologic models were based on concordant beds with the exception of Boyer et al.(2006), based on a natural confluence, and Leite Ribeiro, (2011) and Leite Ribeiro et al., (2012a; b)who supplied sediment only to the tributary in laboratory experiments.

This paperpresents the results of an experimental study on the convergence angle effects on the bed morphology and water surface, on a discordant bed channel confluence with sediment discharge on both channels.

2 METHODOLOGY

Two sets of tests were carried out in an8.5 m long and 0.5 m wide straight glass flume, which represents the main channel. As tributary, a PVC channel which connects with the main one with an angle of 90º (1st set) or 70º (2ndset) was used. The tributary was 4.9 m long and 0.15 m wide (seeFigure 3).

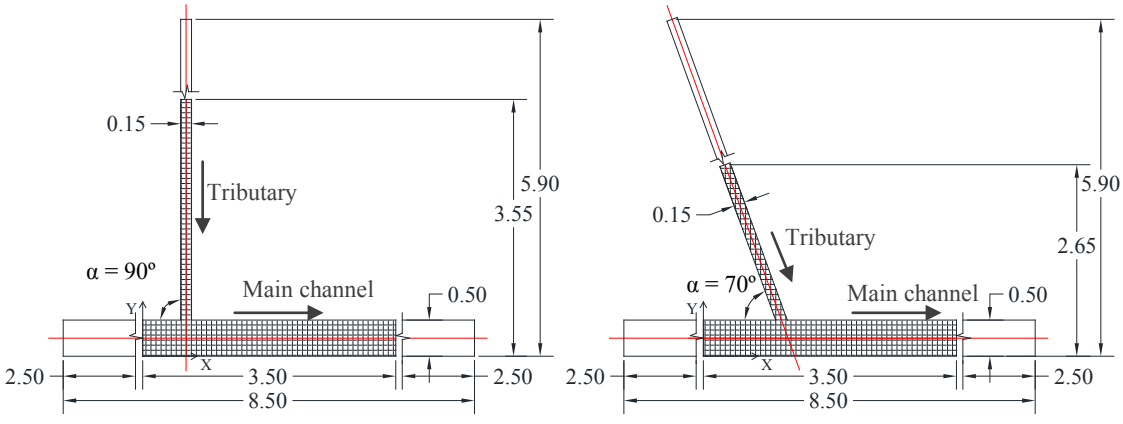

Figure 3 Tested geometric configurations. Left; 90º confluence angle geometry (1st set). Right; 70º confluence angle geometry (2nd set). The shadow area represents the measuring domains.

For each set of tests, three discharge ratioswere tested. The discharge ratio (Q_r) is defined as the ratio between the tributary discharge (Q_t) and the main discharge (Q_m), upstream of the confluence, i.e. $Q_r = Q_t/Q_m$. For all tests, the total post confluence discharge at the ($Q_{p\text{-}c}$) wasset to 30 l/s andkept constant (see Table 1).The three scenarios are hereincalled High, Intermediate and Low (seeTable 1).

Table 1 Tested scenarios

Test n°	Discharge scenario	Q_m [l/s]	Q_t [l/s]	Q_r [-]	α [degrees]	Q_{sm}[kg/min]	Q_{st} [kg/min]
1	High	24.4	5.6	0.23	90º	0.30	0.50
2	Intermediate	26.1	3.9	0.15			
3	Low	27.0	3.0	0.11			
4	High	24.4	5.6	0.23	70º		
5	Intermediate	26.1	3.9	0.15			
6	Low	27.0	3.0	0.11			

During the tests, two types of sediment were used in both channels:

- For the main channel, 0-4 mm sand was used as bed material as well as sediment supply.
- For the tributary, the chosen sediments were a mixture of 80% of 0-4 mm sand and 20% of 4-8 mm gravel.

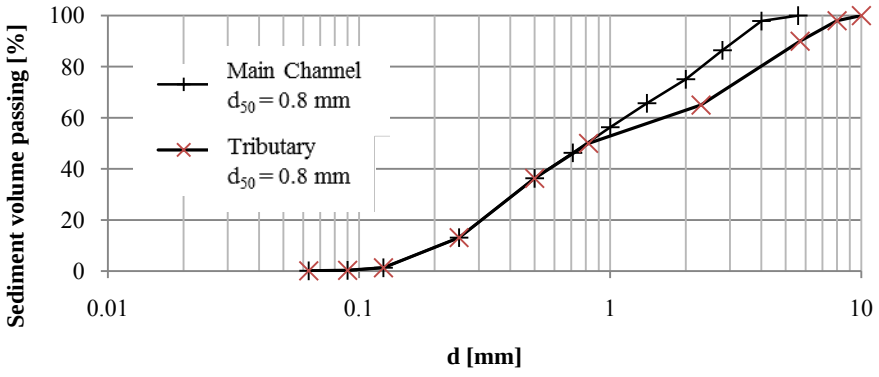

Figure 4 Grain size distributions for supplied sediment into tributary and the main channel

The sediment dischargesadopted were 0.5 kg/minfor the tributary (Q_{st}),and 0.3 kg/min for the main channel (Q_{sm}). Thesesediment discharge capacities were estimated by preliminary calculations based on the Smart & Jaeggi, (1983) and Smart, (1984)sediment transport formula (1):

$$\boldsymbol{Q_b = B_F \times \rho_s \times \frac{4}{s-1} \times R_s \times v_m \times S^{0.6} \times \left(S - \frac{d_m}{12.1 \times R_s}\right) + \left(\frac{d_{90}}{d_{30}}\right)^{0.2}} \quad (1)$$

Where Q_b is the sediment (bed load) discharge in m³/s, B_F is the width of the flume in m, ρ_s is the sediment density (2650 kg/m³), s is the dimensionlesssediment density(ρ_s/ρ_w = 2.65),ρ_w is the water specific weight (ρ_w = 1000 kg/m³)R_s is the hydraulic radio in m, v_m is the mean water velocity, S is the slope of the channel bed, and d_m, d_{90}, and d_{30} are characteristic grain diameters obtained from the grain size distribution of each type of sediments (see Figure 4).

As preliminary hypotheses, a slope between 0.3% and 0.4% was assumed for the main channel and around 1.0% for the tributary. Also, uniform flow in the main channel at the post-confluence reach was assumed; with a uniform depth value of 0.10 m. As the total discharge at the post-confluence was constant ($Q_{p\text{-}c}$ = 30 l/s),v_m was estimated to be 0.60 m/s. For these values, the sediment discharges were computed using (1). Finally, from all obtained values, one was chosen for each flume and kept constant for all the discharge ratios.Table 2summarizes the results for sediments discharge calculations.

Table 2 Main hydraulic values according with the adopted sediment discharges

Discharge Scenario	Discharge Ratio (Q_t/Q_m) [-]	Q_m [l/s]	Q_t [l/s]	Q_{sm} [kg/min]	Q_{st} [kg/min]	Equilibrium Slope (*)	
						Main	Tributary
High	0.23	24.4	5.6	0.30	0.50	0.37%	0.70%
Intermediate	0.15	26.1	3.9			0.35%	0.90%
Low	0.11	27.0	3.0			0.34%	1.00%
(*) These values correspond to the channel bed slopes at equilibrium for the adopted sediment discharges. These values are close to the hypothetical ones.							

To carry out the tests, the channel bed was prepared using the sediments for each flume; sand for the main and mixture sand-gravel for the tributary. At the same time, in order to accelerate the naturally formeddiscordant bed morphology, a step of around 0.03 m was made at the junction between mainchannel and tributary.Also, a slightslope (0.5 %) was built in tributary. This bed morphology does not affect to the final topography because the initial slope and the initial step are smaller than those reached in equilibrium.

Once the channel bed was prepared, the model was slowly filled up with water. Both bed

topographies (tributary and main channel) were measuredjust before starting the test. By comparing the initial bed surface with the one corresponding to the equilibrium state, scour and deposition areas could be identified.

Water level and bed topography surveys were made after 1 and 7 hours of running time and when the equilibrium was reached. Topography measurements were taken by a Mini-Echo-Sounder ± 1mm of accuracy. For water level measurements, an ultrasonic limnimeter (± 1 mm accurate) was used.

The tests were run up to reach the equilibrium, i.e. when the ratio between outgoing and incomingsediment dischargeswas90% or larger. To check the sediment transport rate at the downstream end, the outgoing sediments were weighted periodically, considering them completely saturated. Additionally, equilibrium was also checked by means of topography evolution.

3 RESULTS AND DISCUSSION

3.1. Bed Morphology of the main channel

To analyze the bed morphology patterns, threebed longitudinal profiles are herein consideredand analyzed in detail for each test, corresponding only to the main channel at Y = 0.05; 0.25; 0.45 m (see Figure 5).

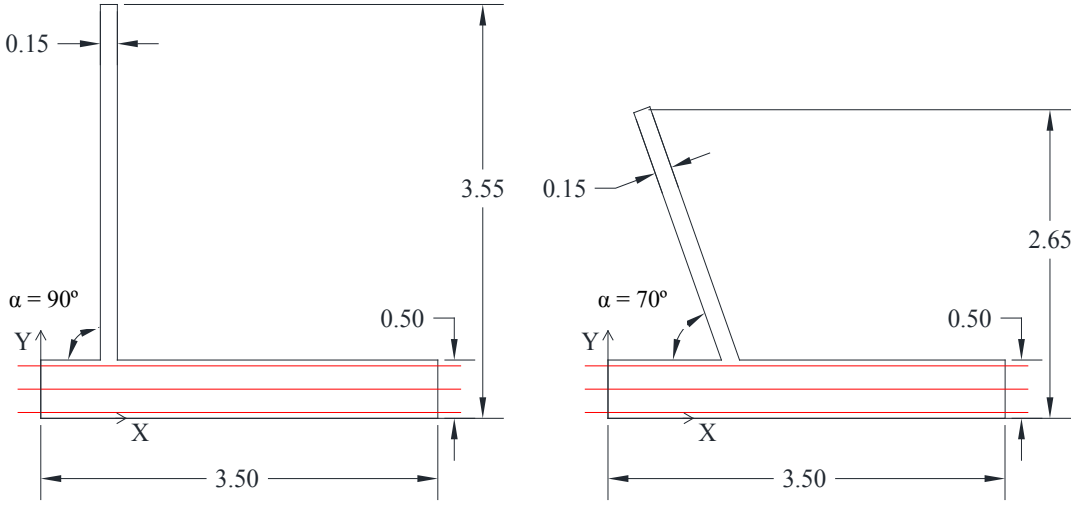

Figure 5 Measurements domains for 90º configuration (left) and 70º configuration (right). Red lines represent the analyzed longitudinal profiles for the main channel.

Figure 6 shows the topography of the 90º confluence for the "Low" discharge ratio. Downstream the confluence, at the inner bank, there is a deposition bar caused by the low water velocities of the flow separation or recirculation zone (see zone 3 in Figure 1). This deposit causes a reduction of the effective flow section, which creates a flow acceleration increasing the water surface slope in this flow region. Starting at the tributary mouth, a main flow corridorrunning around the deposition bar is observed; this eventually reaches the outer wall, where the flowbecomes parallel to the channel axis. This corridor is eroded into the bed, creating a scour area along it and adjacent to the deposition bar (see Figure 6). The general configuration shown in Figure 6 is common for all the experiments, independently of the confluence angle.

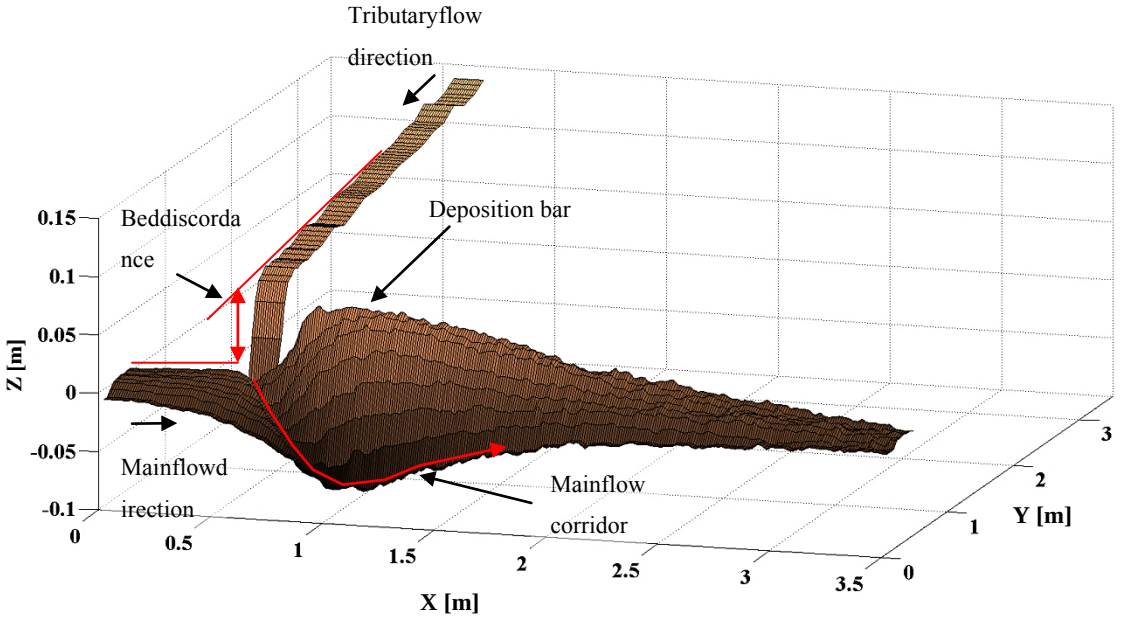

Figure 6 3D view of bed topography for 90º configuration for Q_r = 0.11 (Low), under equilibrium condition.

Figures 7 to 9 show longitudinal topography transepts along the main channel (Y = 0.05, 0.25 and 0.45 m), taken at the end of the experiments, thus when equilibrium condition were reached, for both sets of tests.

Generally, the confluence angle affects the final bed morphology, increasing the above described scour hole both in length and width when changing from 90º to 70º. This is especially true with an increase in the discharge ratio. From figures 7 to 9, a deepening of the scour hole is visible when look at transepts thorough Y = 0.05 and 0.25 m. Furthermore, the length of thescour hole, where the so-called flow corridor runs, increases significantly. As for the deposit located at the inner bank post-confluence region, the so-called separation zone is clearly enhanced by the confluence angle of 70º, when compared to an angle of 90º.

For both confluence angles, an increase in the discharge ratio induces a reduction in the deposit bar. For α = 90º, in the bank transept, the increase of discharge ratio creates an increase in the erosion at the inner bank, which is particularly visible in Figure 9 for the highest Q_r,where a scour hole just in front of the tributary mouth is formed.

Both angle configurations present discordant bed morphology at the end of the tests. Nevertheless, for α = 70º the tributary bed penetrates into the main channel, while for α = 90º the tributary bed penetration is very weak. This is especially evident when looking at transepts Y = 0.45 m, closer to the inner bank, in figures 7 and 8, where an elevation is observed in front of the tributary mouth for 70º angle cases. Moreover, for both angle configurations, the penetration into the main channel increases as the discharge ratio decreases.

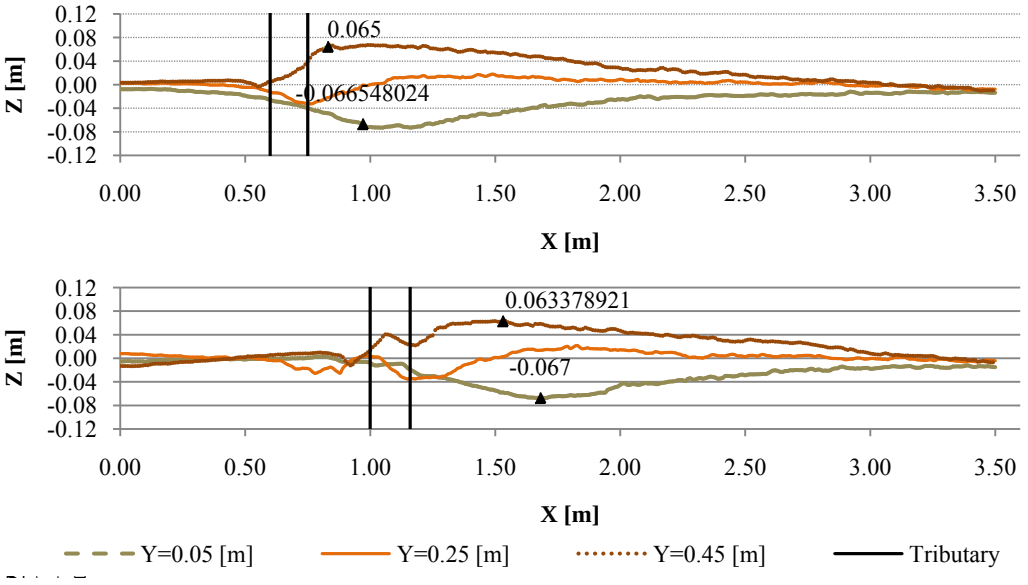

Figure 7 Bed topography longitudinal profiles from the main channel at Y = 0.05; 0.25; and 0.45 m, for the low discharge ratio scenario (Q_r = 0.11), for 90º (upper) and 70º (lower) confluence angles.

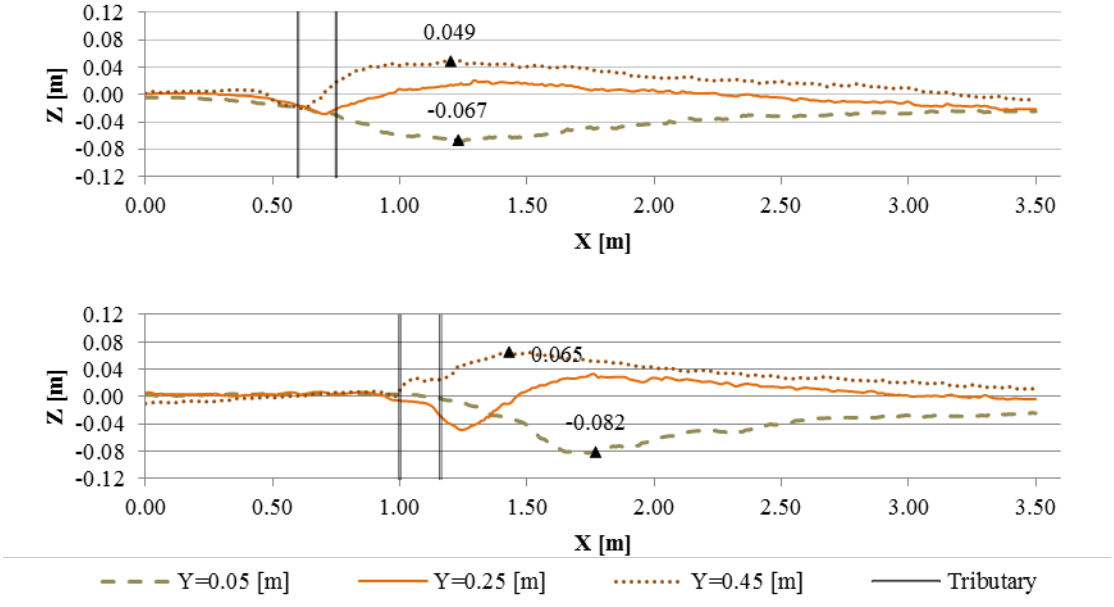

Figure 8 Bed topography longitudinal profiles from the main channel at Y = 0.05; 0.25; and 0.45 m, for the intermediate discharge ratio scenario (Q_r = 0.15), for 90º (upper) and 70º (lower) confluence angles.

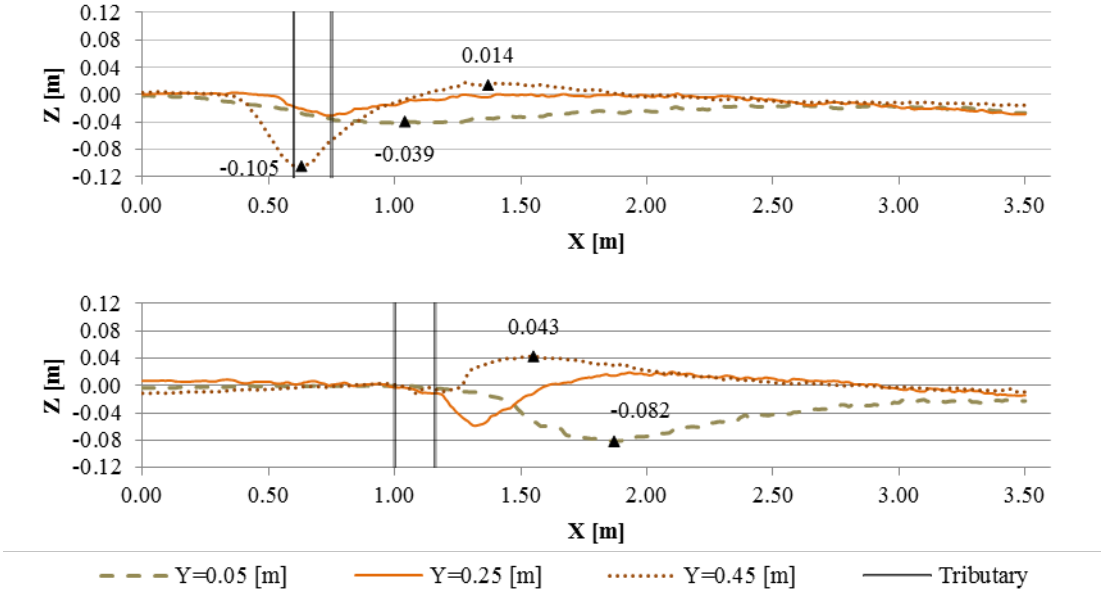

Figure 9 Bed topography longitudinal profilesfrom the main channel at Y = 0.05; 0.25; and 0.45 m,for the high discharge ratio scenario (Q_r = 0.23), for 90º (upper) and 70º (lower) confluence angles.

Some of these morphological features namelythe deposition bar and the bed discordance between main-channel bed and tributary bed, were described previously by Leite Ribeiro, (2011); and Leite Ribeiro et al., (2012a; b). Nevertheless,the corridor herein described was not observed by them in their experiments, where sediments were not supplied in the main channel.

3.2. Water Level of the main channel

To assess the effect of the confluence angle on the water surface, the very same longitudinal profiles as before are selected, corresponding to the main channel.

At the inner bank (Y = 0.45 m), upstream of the confluence, the water level raises up to reach a maximum near the junction(see figures 10 to 12). This increase coincides with the stagnation zone where the water velocities are very low and the decreaseof kinetic energy is compensated by anincrease inthe water level (piezometric term). At the same time, at the axis and at the outer bank (Y = 0.25 m and Y = 0.05 m), the water level remains almost unchanged until reaching the confluence, reflecting a sub-critical back water effectimposed by the confluence (singularity in the flow) which reduces the energy slope (see figures 10 to 12).

Downstream of the confluence, the flow is mainly characterized by a clear acceleration induced by the reduction of the effective flow cross section associated with the deposition bar placed at the inner bank, just downstream of the confluence. This flow acceleration causes an increase in the slope of the water surface downstream of the confluence (see figures 10 to 12).

The confluence angle effects on the water surface consist on a downstream displacement of the water level drop caused by the flow junction. For α = 90º, this drop is registered before or within the junction zone, while for α = 70º, the drop is registered downstream of the junction. In this configuration, the water level drop seems to increase its magnitude as the discharge ratio increases, while the opposite occurs for α = 90º (see figures 10 to 12).Moreover, the profiles measured at the channel axis (Y = 0.25 m) and at the outer bank (Y = 0.05 m), exhibit, especially for the low discharge ratio, a water level raise similar to the one observed at the inner bank for α = 90º. This effect is not observed for α = 70º, in which the water level at the channel axis and at the outer bank remain almost horizontal until reaching the confluence. This fact indicates that the stagnation zone is wider in the case of the 90º angle configuration (see figures 10 to 12).

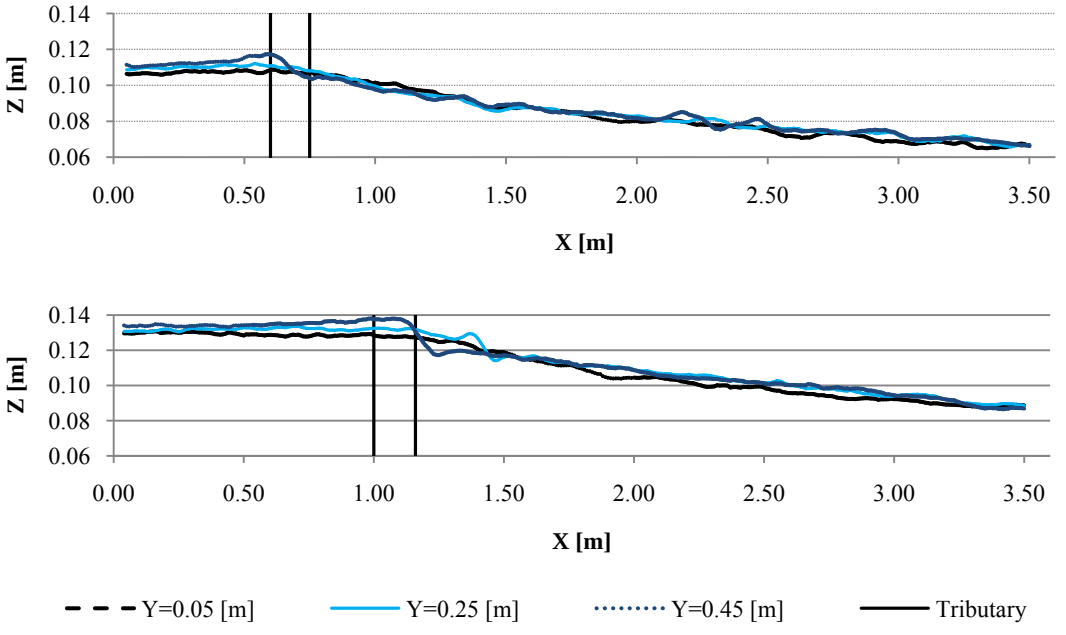

Figure 10 Water level longitudinal profiles from the main channel at Y = 0.05; 0.25; and 0.45 m,for the low discharge ratio scenario (Q_r = 0.11), for 90º (upper) and 70º (lower) confluence angles.

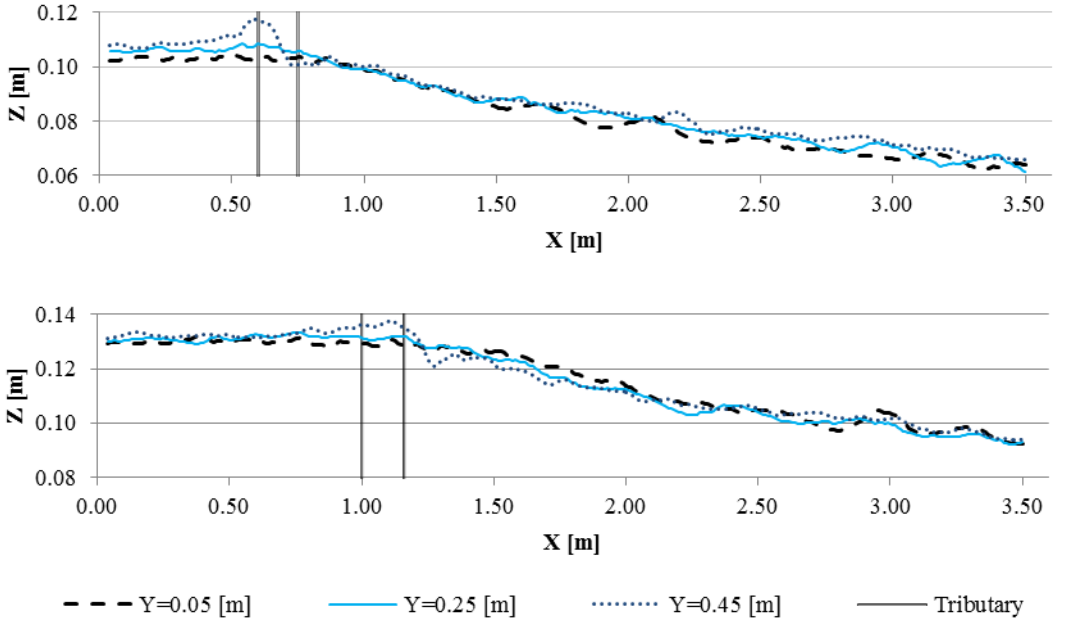

Figure 11 Water level longitudinal profiles from the main channel at Y = 0.05; 0.25; and 0.45 m, for the intermediate discharge ratio scenario (Q_r = 0.15), for 90º (upper) and 70º (lower) confluence angles.

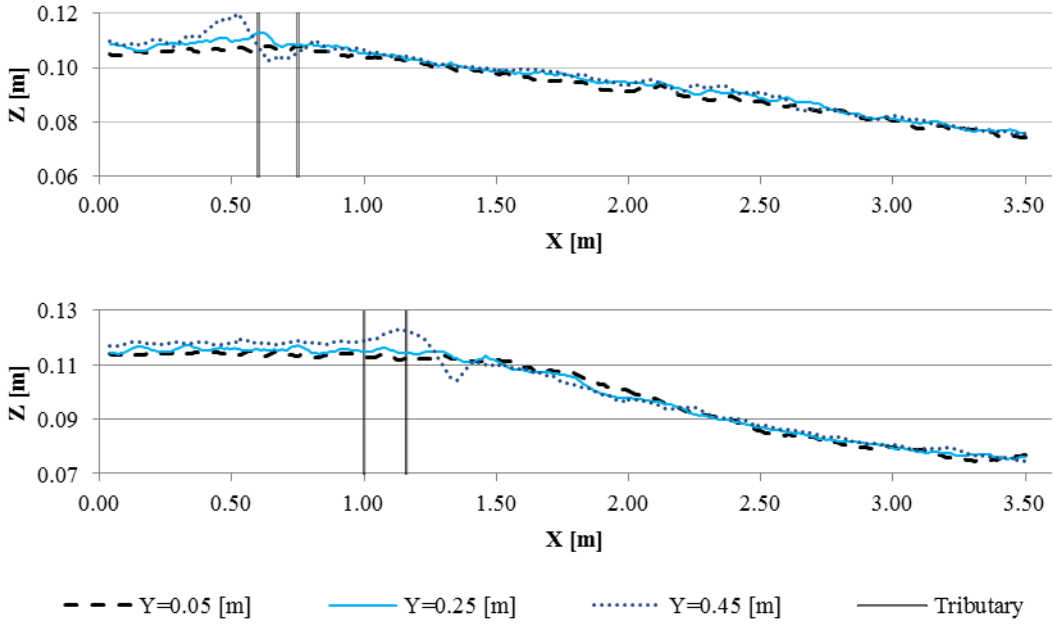

Figure 12 Water level longitudinal profiles from the main channel at Y = 0.05; 0.25; and 0.45 m, for the high discharge ratio scenario (Q_r = 0.23), for 90º (upper) and 70º (lower) confluence angles.

Froude numbersare determined for both channels considering the mean water depth (h_m) and flow velocity (v_m) upstream and downstream of the confluence.Tables 3 and 4show these values for each discharge ratio and for α = 90º and α = 70º, respectively. The tributary flow regime is different depending on the confluence angle.For α = 90º, the tributary flow is critical or super-critical (Fr ≥ 1) for all the discharge ratios(see Table 3). For this geometry configuration, the Froude number corresponding to the tributary flow decreases as the discharge ratio increases (see Table 3).Furthermore, for α = 70º, the Froude number is smaller than 1 for all the discharge ratios, increasing in value as the discharge ratio increases (see Table 4).

Table 3 Values of main hydraulic variables for tributary and main channel flows for α = 90º. Main channel values are considered upstream of the confluence. h_m is the mean water depth and v_m is the mean flow velocity.

Discharge ratio scenario	Q_t[l/s]	Q_m [l/s]	Q_r [-]	Tributary 90º			Main upstream 90º			Main downstream 90º		
				h_m [m]	v_m[m/s]	**Froude**	h_m [m]	v_m [m/s]	**Froude**	h_m [m]	v_m [m/s]	**Froude**
Low	3.0	27.0	0.11	0.028	0.72	**1.37**	0.109	0.50	**0.48**	0.075	0.80	**0.93**
Intermediate	3.9	26.1	0.15	0.036	0.72	**1.21**	0.105	0.50	**0.49**	0.081	0.74	**0.82**
High	5.6	24.4	0.23	0.052	0.71	**1.00**	0.102	0.48	**0.48**	0.075	0.80	**0.94**

As the flow regime in the main channel is always sub-critical (Fr < 1) upstream and downstream of the confluence, for α = 90º a hydraulic jump is observed at the junction of both flows (not shown here). The hydraulic jump becomes weaker as the discharge ratio increases. On the contrary, for α = 70º, there is a local increase of the water level that becomes larger as the discharge ratio increases.

Table 4 Values of main hydraulic variables for tributary and main channel flows for α = 70º. Main channel values are considered upstream of the confluence. h_m is the mean water depth and v_m is the mean flow velocity

Discharge ratio scenario	Q_t[l/s]	Q_m [l/s]	Q_r [-]	Tributary 70º			Main upstream 70º			Main downstream 70º		
				h_m [m]	v_m[m/s]	**Froude**	h_m [m]	v_m [m/s]	**Froude**	h_m [m]	v_m [m/s]	**Froude**
Low	3.0	27.0	0.11	0.060	0.33	**0.44**	0.132	0.41	**0.36**	0.10	0.63	**0.65**
Intermediate	3.9	26.1	0.15	0.055	0.47	**0.64**	0.131	0.4	**0.35**	0.10	0.60	**0.61**
High	5.6	24.4	0.23	0.062	0.60	**0.77**	0.115	0.42	**0.40**	0.09	0.67	**0.72**

For α = 70º, the sub-critical flow regime at the tributary indicates that the main channel subcritical flowregime is imposedalong the tributary, constituting the downstream boundary condition of the tributary flow.For α = 90º, the tributary flow is integrated into the main flow through a hydraulic jump, which may be associated to a scour hole observed at the tributary mouth (not shown here), and a slight flow deflection towards the outer bank that excavates a main corridor around the deposition bar until reaching the outer bank. For this angle configuration the hydraulic jump predominates over the flow deflection, creating a deeper scour hole at the tributary mouth as discharge ratio increases.On the contrary, for α = 70º, as the tributary flow regime is sub-critical, there is no hydraulic jump at the confluence andthe flow deflection plays a predominant role creating a main flow corridor around the deposition bar deeper as closer to the outer bank (see figures 7 to 9).

4 CONCLUSIONS

The convergence angle is a factor that strongly influences on the hydro-morphodynamic of channel confluences. As detailed in this paper, different bed morphology and water surface patterns have been identified for two different confluence angles and three discharge ratios (Q_r).

After six experimental tests with feeding sediment in the tributary as well as in the main channel, some morphological features were identified as characteristics of bed topography at channel confluences for both angle configurations and all discharge ratios. These are bed discordance, deposition bar and scour area or main flow corridor. Some of them,namelydeposition bar and bed discordance, match with the results obtained by Leite Ribeiro, (2011); and Leite Ribeiro et al., (2012a; b). However, the main flow corridor, downstream of the confluence, constitutes a difference when compared with their results where no important scour holes were observed.Also, from water level measurements, some of the main flow dynamic features, according to Best,(1987) (Figure 1), like flow stagnation, maximum velocity and flow separation or recirculation zone were identified. Moreover, a hydraulic jump was observed at the tributary mouth for α = 90º.

Different convergence angle geometries cause erosions at different places of the main channel bed. For α = 90º, the deepest erosion is placed close to the inner wall, and becomes deeper as the discharge ratio increase; whereas for α = 70º, the deepest erosion is registerednear to the outer wall, being deeperas discharge ratio increase. Also, the deposition bar, associated to the flow separation zone is more developed for 70º (see Figure9).

In addition, the convergence angle affects to the confluence flow dynamic by reducing the width of the flow stagnation zone when it changes from 90º to 70º. Also, the water surface drop caused by the flow junction is displaced downstream of the confluence for α = 70º, and the drop height increases as the flow ratio increases.While for α = 90º the head loss occurs upstream or within the junction, reducing the drop height as the flow ratio increases. Different confluence angles causes different flow regimes in the tributary, which is critical or super-critical for α = 90º and sub-critical for α = 70º.

Different flow regimes at the tributary, lead to think that the influence of the flows on each other is different depending of the angle configuration. For a better understanding of this phenomenon, further investigations, like velocity fields, are needed.

ACKNOWLEDGEMENT

This research is developed within the framework of the Joint Doctoral Initiative IST-EPFL. Funded by FCT and LCH/EPFL. Contract reference no. SFRH/BD/51453/2011.

References

Best, J. L. 1987. Flow dynamics at river channel confluences: Implications for sediment transport and bed morphology. Recent Developments in Fluvial Sedimentology, Spec. Publ. SEPM Soc. Sediment. Geol., (39), 27–35.

Best, James L. 1988. Sediment transport and bed morphology at river channel confluences. Sedimentology, 35(3), 481–498.

Best, James L, & Rhoads, B. L. 2008. Sediment Transport, Bed Morphology and the Sedimentology of River Channel Confluences. River Confluences, Tributaries and the Fluvial Network (pp. 45–72). John Wiley & Sons, Ltd.

Biron, P., Best, J. L., & Roy, A. G. 1996. Effects of Bed Discordance on Flow Dynamics at Open Channel Confluences. Journal of Hydraulic Engineering, 122(12), 676–682.

Biron, P. M., Richer, A., Kirkbride, A. D., Roy, A. G., & Han, S. 2002. Spatial patterns of water surface topography at a river confluence. Earth Surface Processes and Landforms, 27(9), 913–928.

Boyer, C., Roy, A. G., & Best, J. L. 2006. Dynamics of a river channel confluence with discordant beds: Flow turbulence, bed load sediment transport, and bed morphology. J. Geophys. Res., 111(F4), F04007.

Bradbrook, K. F., Biron, P. M., Lane, S. N., Richards, K. S., & Roy, A. G. 1998. Investigation of controls on secondary circulation in a simple confluence geometry using a three-dimensional numerical model. Hydrological Processes, 12(8), 1371–1396.

Bradbrook, K. F., Lane, S. N., Richards, K. S., Biron, P. M., & Roy, A. G. 2001. Role of Bed Discordance at Asymmetrical River Confluences. Journal of Hydraulic Engineering, 127(5), 351–368.

Fujita, I., & Komura, S. 1989. Visualization of the Flow at a Confluence. Proceedings of the International Symposium on Refined Flow Modelling and Turbulence Measurements, Tokyo, Japan (pp. 517–524).

Leite Ribeiro, M. 2011. Influence of Tributary Widening on Confluence Morphodynamics. Ecole Polytechnique Fédérale de Lausanne, Lausanne, Switzerland, Thesis No. 4951. Communication (LCH) No 46.

Leite Ribeiro, M., Blanckaert, K., Roy, A. G., & Schleiss, A. J. 2012a. Hydromorphological implications of local tributary widening for river rehabilitation. Water Resources Research, 48(10), 1–19.

Leite Ribeiro, M., Blanckaert, K., Roy, A. G., & Schleiss, A. J. 2012b. Flow and sediment dynamics in channel confluences. Journal of Geophysical Research: Earth Surface, 117(F1), 1–19.

Mosley, M. P. 1976. An Experimental Study of Channel Confluences. The Journal of Geology, 84(5), 535–562.

Parsons, D. R., Best, J. L., Lane, S. N., Orfeo, O., Hardy, R. J., & Kostaschuk, R. 2007. Form roughness and the absence of secondary flow in a large confluence–diffluence, Rio Paraná, Argentina. Earth Surface Processes and Landforms, 32(1), 155–162.

Rhoads, B. L., & Kenworthy, S. T. 1997. Time-averaged flow structure in the central region of a stream confluence. Earth Surface Processes and Landforms, 23(2), 171–191.

Smart, G. 1984. Sediment Transport Formula for Steep Channels. Journal of Hydraulic Engineering, 110(3), 267–276.

Smart, G. M., & Jaeggi, M. 1983. Sediment Transport on Steep Slopes. Mitteilungen der Versuchsanstalt fuer Wasserbau, Hydrologie und Glaziologie (VAW), Eidgenossische Technische Hochschule (ETH), Zurich,Mitteilung No. 64.

Weber, L. J., Schumate, E. D., & Mawer, N. 2001. Experiments on flow at a 90 degrees open-channel junction. J Hydraulic Engineering, 127(5), 340–350.